Virginia Tech Interlibrary Loan

Electronic Delivery Cover Sheet

NOTICE WARNING CONCERNING COPYRIGHT RESTRICTIONS

The copyright law of the United States (Title 17, United States Code) governs the making of photocopies or other reproductions of copyrighted materials.

Under certain conditions specified in the law, libraries and archives are authorized to furnish a photocopy or other reproduction. One of these specified conditions is that the photocopy or reproduction is not to be "used for any purpose other than private study, scholarship, or research." If a user makes a request for, or later uses, a photocopy or reproduction for purposes in excess of "fair use," that user may be liable for copyright infringement.

This institution reserves the right to refuse to accept a copying order if, in its judgment, fulfillment of the order would involve violation of copyright law.

This notice is posted in compliance with
Title 37 C. F. R., Chapter II, Part 201.14

International Journal of Mining, Reclamation and Environment

ISSN: 1748-0930 (Print) 1748-0949 (Online) Journal homepage: http://www.tandfonline.com/loi/nsme20

Specific conductivity sensor performance: II. Field evaluation

Travis P. Maupin , Carmen T. Agouridis , Dwayne R. Edwards , Christopher D. Barton , Richard C. Warner & Michael P. Sama

To cite this article: Travis P. Maupin , Carmen T. Agouridis , Dwayne R. Edwards , Christopher D. Barton , Richard C. Warner & Michael P. Sama (2013) Specific conductivity sensor performance: II. Field evaluation, International Journal of Mining, Reclamation and Environment, 27:5, 345-365, DOI: 10.1080/17480930.2013.764702

To link to this article: http://dx.doi.org/10.1080/17480930.2013.764702

International Journal of Mining, Reclamation and Environment, 2013
Vol. 27, No. 5, 345–365, http://dx.doi.org/10.1080/17480930.2013.764702

Taylor & Francis
Taylor & Francis Group

Specific conductivity sensor performance: II. Field evaluation

Travis P. Maupin[a], Carmen T. Agouridis[b]*, Dwayne R. Edwards[b], Christopher D. Barton[c], Richard C. Warner[b] and Michael P. Sama[b]

[a]*Strand Associates, Inc., Columbus, IN, USA;* [b]*Biosystems Agricultural Engineering Department, University of Kentucky, Lexington, KY, USA;* [c]*Forestry Department, University of Kentucky, Lexington, KY, USA*

(*Received 4 September 2012; final version received 8 January 2013*)

The US Environmental Protection Agency (USEPA) has issued guidance on the specific conductivity ($EC_{25°C}$) of waters discharged from mined lands in the Appalachian Coal Belt Region of the USA. In this guidance, the USEPA states that these waters should have an $EC_{25°C}$ less than 300–500 μS cm^{-1}. Such a requirement places great importance on accurately determining $EC_{25°C}$. Building upon a laboratory-based evaluation of four types of commercially available continuous logging conductivity sensors, this study examined sensor performance in the more harsh and variable field environments at forested and mined land streams in eastern Kentucky. The objectives of this study were to calculate the white noise variance associated with each sensor type and to evaluate white noise variance in relation to variations in $EC_{25°C}$ and discharge. Results of the study indicate that predominant increases in $EC_{25°C}$, and to some extent increases in discharge, explain between 35 and 65% of the white noise variance.

Keywords: coal mining; Appalachia; water quality; conductivity; white noise

Introduction

Water quality characteristics fluctuate in response to changes in environmental factors such as precipitation, land use, time of day (diurnal) and season or climate [1–4]. In order to adequately account for these variations in water quality, continuous water quality monitoring is recommended [5,6]. Such high frequency *in situ* monitoring is best suited for capturing cyclical trends associated with seasons or diurnal fluctuations as well as rapid changes associated with storm events [7,8]. But which continuous water quality monitoring sensors to select becomes a challenging question. Sensor selection is dependent on a number of variables including project objectives, monitoring site conditions, sensor construction and ruggedness, accuracy and precision requirements and budget [5,9]. In some cases, data from one water quality parameter can serve as a surrogate for another water quality parameter [5]. Turbidity and electrical conductivity (EC) are two such examples whereby a continuously recorded parameter is used to predict levels for variables that are more expensive and time consuming to measure. Studies have demonstrated that turbidity is a viable surrogate for total suspended solids [10–12]

*Corresponding author. Email: carmen.agouridis@uky.edu

and total phosphorus [11,13] while EC can serve as a surrogate for total dissolved solids (TDS) [10,14,15].

Within the Appalachian Coal Belt Region of the USA, the issue of EC has gained importance due to the realised impact of coal mining on stream water quality and biotic composition. Note that EC is temperature corrected to 25 °C, and thus termed specific conductivity ($EC_{25°C}$), so that values are comparable between locations and across time. Research has demonstrated that elevated levels of TDS, and hence EC, negatively impact aquatic life. Pond et al. [4] found that when $EC_{25°C}$ levels were greater than 500 μS cm^{-1}, Ephemeroptera communities were negatively impacted in the Appalachian Coal Belt Region. Pond [16] also found a negative correlation between Plecoptera and Trichoptera communities and $EC_{25°C}$ in this region. The results of these studies and others in the region [17–19] prompted the US Environmental Protection Agency (USEPA) to issue guidance stating that waters discharged from mines in the Appalachian Coal Belt Region should have $EC_{25°C}$ levels below 300–500 μS cm^{-1} [20]. Therefore, accurately determining the $EC_{25°C}$ levels of mine discharged water is of great importance to the USEPA and mine operators alike. Equally important is understanding the range in $EC_{25°C}$ values that at occurs in discharged waters, which is possible with continuous monitoring and not just a point in time, which occurs with a grab sample. It is entirely possible for a stream to have a typical $EC_{25°C}$ level above 300–500 μS cm^{-1} but show a lower value due to dilution from run-off produced during a storm event entering the stream. A grab sample would not reveal this trend whereas continuous monitoring would.

Maupin et al. [21] in a controlled laboratory study found variations in performance, between four types of continuous recording conductivity sensors (YSI 6600 V2-4 sonde, HOBO U-24-001, Solinst Model 3001 LTC Levelogger Junior, and In-Situ Aqua TROLL 100), with regards to temporal stability (i.e. consistency) and accuracy. Examining 42 temperature and $EC_{25°C}$ combinations, the authors found that only three of the four sensors output consistent $EC_{25°C}$ measurements over time with temporal fluctuations greatest at the highest $EC_{25°C}$ standard (10,000 μS cm^{-1}). With regards to accuracy, the HOBO tended to overestimate $EC_{25°C}$ while the other sensors tended to underestimate $EC_{25°C}$ for the range of 5–9986 μS cm^{-1}. However, for the range of 5–1411 μS cm^{-1}, which represents conditions more frequently found in streams, the YSI tended to over-predict $EC_{25°C}$ and the Aqua TROLL tended to underpredict $EC_{25°C}$. Furthermore, at least one sensor within each sensor type performed quite differently than the other sensors of the same type. This result indicates that individual sensors should be examined carefully before deployment.

Because the study by Maupin et al. [21] was performed in a controlled environment, care must be taken when extrapolating results to field conditions as these are more harsh and variable than a laboratory setting. Though Wagner et al. [5] noted that conductivity sensors are typically reliable and durable, they are susceptible to fouling from biofilms, sediment and ion precipitants. Fritz et al. [22] measured elevated levels of $EC_{25°C}$ and dissolved constituents in waters discharged from valley fills in the Appalachian Coal Belt Region. When compared to waters discharged from reference forested watersheds, average concentrations of SO_4^{2-}, Cl^-, Mn, Mg^{2-}, Fe and Ca^{2+} in waters discharged from valley fills were about 108, 3, 145, 73, 69 and 9 times greater, respectively. Average $EC_{25°C}$ values were about 45–65 times greater. In the presence of such elevated constituent concentrations, sensor fouling and thus sensor accuracy becomes a concern [23]. Furthermore, $EC_{25°C}$ levels in streams can change rapidly as discharges fluctuate with values of $EC_{25°C}$; $EC_{25°C}$ levels tend to decrease with increasing

discharge [1,3]. The correlation is of importance in mined areas where hydrographs associated with valley fills are more peaked than unmined sites [24,25]. This means that conductivity sensors must have the capability of accurately recording $EC_{25°C}$ levels under a wide range of water quality and flow conditions.

The purpose of this study was to compare the field performance of four commercially available continuously logging conductivity sensors in both mined and unmined streams. The objectives of this study were to: (1) calculate the white noise variance associated with each sensor type and (2) evaluate white noise variance in relation to variations in $EC_{25°C}$ and discharge.

Methods

Sensor description

Four conductivity sensors were evaluated in this study: YSI 6600 V2-4 data sonde (YSI Incorporated, Yellow Springs, OH, USA), HOBO U-24-001 (Onset Computer Corporation, Cape Cod, MA, USA), Solinst Model 3001 LTC levelogger Junior (Solinst Canada Ltd, Georgetown, Ontario, Canada) and In-Situ Aqua TROLL 100 (In-Situ Incorporated, Fort Collins, Co., USA). Henceforth, these sensors will be referred to as YSI, HOBO, Solinst and Aqua TROLL, respectively. For a description of the operating parameters, calibration techniques and manufacturer information for each sensor, see Maupin et al. [21].

Study sites

The study sites are located within the University of Kentucky's Robinson Forest. Robinson Forest is a 6100-ha second-growth forest located in Cumberland Plateau in south-eastern Kentucky. In the mid-1990s, a portion of Robinson Forest was mined for coal resulting in the creation of valley fills. On one of these valley fills (Guy Cove), ephemeral, intermittent and perennial stream channels were created totaling about one mile in length [26]. As expected with different land uses, water quality characteristics of streams flowing through Robinson Forest vary considerably. For 2011, $EC_{25°C}$ levels in forested reaches averaged about 40 $\mu S\ cm^{-1}$; those on the restored reach of Guy Cove varied from 450 to 850 $\mu S\ cm^{-1}$; and those at the outlet of valley fills averaged about 1700–2100 $\mu S\ cm^{-1}$ [27]. Such variation is ideal for field-testing conductivity sensors.

Three locations of widely varying water quality and discharge were selected to test the conductivity sensors: Little Millseat (LMS), Guy Cove 01 (GC01) and Guy Cove 03 (GC03) [27]. The average cation and anion concentrations at the sites in 2011 are presented in Table 1. Table 2 contains average nutrient and metal concentrations in 2011 for the three sites. The LMS location was at the outlet of a 90+-year-old second-growth forested watershed that is about 75.7 ha in size. The GC01 and GC03 locations were located at the start and end of a stream creation project, respectively (Figure 1). Although the 9.2 ha watershed above the GC01 location was not mined, trees were harvested when the surrounded area was mined in the mid-1990s. As seen in Figure 1, the forest above GC01 has regrown considerably since it was harvested. The GC03 location is at the toe or outlet of the valley fill. This location receives waters primarily from the underdrain but also from the upgradient recreated intermittent and ephemeral streams. GC03 also receives run-off from 43.6 ha of lands that were mostly traditionally reclaimed though about 4 ha was reclaimed using the Forestry Reclamation Approach.

Table 1. Mean and standard deviation of cation and anion concentrations in water samples from the 2011 monitoring year.[a]

Site[b]	$EC_{25°C}$ ($\mu S\ cm^{-1}$)	Cl^- ($mg\ L^{-1}$)	SO_4^{2-} ($mg\ L^{-1}$)	Mg ($mg\ L^{-1}$)	Ca^{2+} ($mg\ L^{-1}$)	K^+ ($mg\ L^{-1}$)	Na^+ ($mg\ L^{-1}$)
LMS	43 ± 11	1.3 ± 1.3	15 ± 2.7	1.7 ± 0.4	2.5 ± 1.0	1.3 ± 0.8	1.3 ± 0.4
GC01	457 ± 144	2.4 ± 2.2	417 ± 457	47 ± 28	24 ± 19	5.8 ± 1.9	3.9 ± 1.1
GC03	1724 ± 346	2.5 ± 0.9	1780 ± 526	180 ± 51	91 ± 58	8.8 ± 1.7	10.0 ± 2.8

[a]Sample period: from January 2011 to November 2011.
[b]LMS = Little Millseat ($n = 49$); GC01 = Guy Cove 01 ($n = 18$); and GC03 = Guy Cove 03 ($n = 18$).

Table 2. Mean and standard deviation of nutrient and metal concentrations in water samples from the 2011 monitoring year.[a]

Site[b]	pH (su)	NO_3^- ($mg\ L^{-1}$)	NH_4^+ ($mg\ L^{-1}$)	Alkalinity ($mg\ L^{-1}$)	Fe ($mg\ L^{-1}$)	Mn ($mg\ L^{-1}$)
LMS	6.6 ± 0.2	0.11 ± 0.01	0.09 ± 0.01	33 ± 21	0.04 ± 0.02	0.26 ± 0.2
GC01	7.8 ± 0.2	0.17 ± 0.1	0.10 ± 0.2	509 ± 174	–	–
GC03	6.6 ± 0.1	0.01 ± 0.01	0.15 ± 0.2	91 ± 28	–	–

[a]Sample period: from January 2011 to November 2011.
[b]LMS = Little Millseat ($n = 49$); GC01 = Guy Cove 01 ($n = 18$); and GC03 = Guy Cove 03 ($n = 18$).

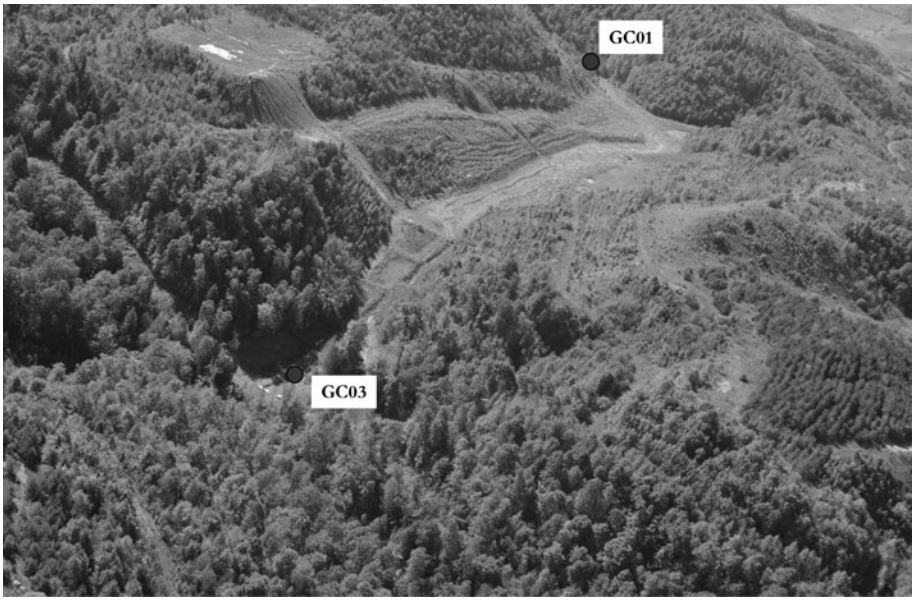

Figure 1. Conductivity sensor field study sites.
Locations identified with red circle. GC01 = Guy Cove 01; GC03 = Guy Cove 03; Little Millseat (LMS) not shown.

The 43.6 ha watershed up-gradient of GC03 is strongly influenced by discharge from the underdrain. Both the LMS and GC01 locations were fully shaded while the GC03 location was partially shaded.

Data collection

Specific conductivity

The same conductivity sensors used in Maupin et al. [21] were used in this study. Prior to deployment, each sensor was calibrated per manufacturer's recommendations. At each site, all conductivity sensors were deployed in riffles such that the sensors were fully submerged. The sensors were placed in riffles to ensure steady flow over the sensors and to prevent sediment deposition in the sensor housing. The HOBO, Solinst and Aqua TROLL sensors were each housed in their own 5-cm diameter PVC pipes for protection. These white PVC pipes allowed flows to continuously circulate through the housing units and across the sensors. To avoid the potential for fouling due to metal contact, these sensors were secured in the PVC pipe using plastic zip ties. The YSI sensors were protected in manufacturer supplied dark grey deployment cases. It is possible that the colour of the housing units had an effect on temperature readings even though the sites were either fully shaded or partially shaded; however, examination of temperature data from the sensors revealed no appreciable differences.

During the project period, the conductivity sensors recorded $EC_{25°C}$ and temperature data for seven deployment periods. The length of the deployment periods varied, but generally encompassed a period of 2–3 weeks (range was 10–28 days with an average of 20 days). Data were collected at 15-min intervals. Conductivity sensors were not rotated between sites but remained at the same site throughout the study. Between each deployment, conductivity sensors were cleaned and recalibrated, as required, per manufacturer's recommendations. Budgetary constraints and another project need prevented the use of all conductivity sensors at all deployments. As part of an undergraduate course, the YSI sensors were periodically used to monitor the water quality of streams in the Lexington, Kentucky area. None of these streams have any known metal

Table 3. Conductivity sensor deployment schedule.

	Deployment[a]						
Sensor/location	1	2	3	4	5	6	7
YSI							
LMS	X	X	X	X		X	
GC01	X			X			X
GC03	X	X	X	X			X
HOBO							
LMS	X	X	X	X	X	X	X
GC01	X	X	X	X	X	X	X
GC03	X	X	X	X	X	X	X
Solinst							
LMS				X	X	X	
GC01				X	X	X	X
GC03				X	X	X	X
Aqua TROLL							
LMS				X	X	X	X
GC01				X	X	X	X
GC03				X	X	X	X

[a]Deployment periods: 1 = 16 March 2011–1 April 2011 (17 days); 2 = 14 April 2011–5 May 2011 (22 days); 3 = 19 May 2011–29 May 2011 (11 days); 4 = 23 June 2011–13 July 2011 (21 days); 5 = 28 July 2011–17 August 2011 (21 days); 6 = 8 September 2011–6 October 2011 (29 days) for HOBO, Solinst and Aqua Troll and 8 September 2011–28 September 2011 (21 days) for YSI; and 7 = 28 October 2011–20 November 2011 (23 days) for HOBO, Solinst and Aqua Troll and 28 October 2011–17 November 2011 (21 days) for YSI.

contamination issues, and as such, did not affect the performance of the YSI sensors. The Solinst and Aqua TROLL sensors were not deployed until period 4 as they were not purchased until the spring of 2011. Table 3 notes the location and deployment period for each conductivity sensor used in the study.

Discharge

Because of the expected influence of discharge on $EC_{25°C}$ levels, flow was measured at each of the three study sites. At GC01 and GC03, discharge was continuously measured using trapezoidal flumes [28] and In-Situ Level Trolls (5 psig) pressure transducers (Fort Collins, CO). Water level data were collected at 15-min intervals. At LMS, discharge data were continuously recorded using a 3:1 side-sloped broad-crested combination weir and In-Situ Level Troll (5 psig) pressure transducer [29].

Data analysis

White noise

Because $EC_{25°C}$ values measured in the field could not be compared to known $EC_{25°C}$ standards, as was the case in the controlled laboratory study reported by Maupin et al. [21], and since the accuracy and resolution of the sensors varied slightly, a white noise analysis was performed to assess temporal variations in the conductivity sensor readings [30]. White noise is useful in modelling the impact of random disturbances, such as sensor noise (e.g. error associated with changes in voltage) and environmental disturbances (e.g. storm events and temperature changes), on sensor output (i.e. $EC_{25°C}$ readings). As noted by Kenny [31], when the noise of the sensor becomes greater than the fluctuations in the electrical signal produced by the physical phenomenon, then the performance of the sensor is limited. Evaluating white noise variance aids in the understanding of sensor performance over time. The goal of the analysis was to determine if the variance of the white noise differed between sensor types and location and if it was related to $EC_{25°C}$ and discharge. Since variation in the white noise was desired, grouping of the data into time blocks was required to permit the computation of variance. For each study site and deployment period, a time block of three hours was used. A time block of three hours was chosen as it provided a representative time sample (e.g. enough data points) while maintaining a constant variance of $EC_{25°C}$ within the blocks. As $EC_{25°C}$ and flow data were collected at 15-min intervals, each time block consisted of 12 data points.

Equation (1) was used to model white noise for each $EC_{25°C}$ data point.

$$a(d) = X'(d) - [\rho * (X'(d-1)] \tag{1}$$

The variable $a(d)$ is the white noise associated with each data point, d (μS cm^{-1}); $X'(d)$ is the detrended sensor output for each data point (μS cm^{-1}); and ρ is the lag 1 autocorrelation coefficient.

Because white noise analysis requires normally distributed data, the $EC_{25°C}$ data were detrended by subtracting the trend line ($EC_{25°C}$ versus time) from each data point, $X(d)$, using Equation (2).

$$X'(d) = X(d) - \alpha - \beta d \tag{2}$$

The variables α and β are the intercepts and the slopes, respectively, of the best-fit lines for each sensor and deployment period (e.g. YSI sensor at GC01 and deployment period 1). Figure 2 shows the original and detrended $EC_{25°C}$ data, respectively, for a one 3-h time block. Once the $EC_{25°C}$ data were detrended, the lag 1 autocorrelation coefficient, ρ, was calculated using Equation (3) to detect non-randomness in the data.

$$\rho(\tau) = \frac{\mathrm{Cov}(X(d), X(d+\tau))}{\mathrm{Var}(X(d))} \tag{3}$$

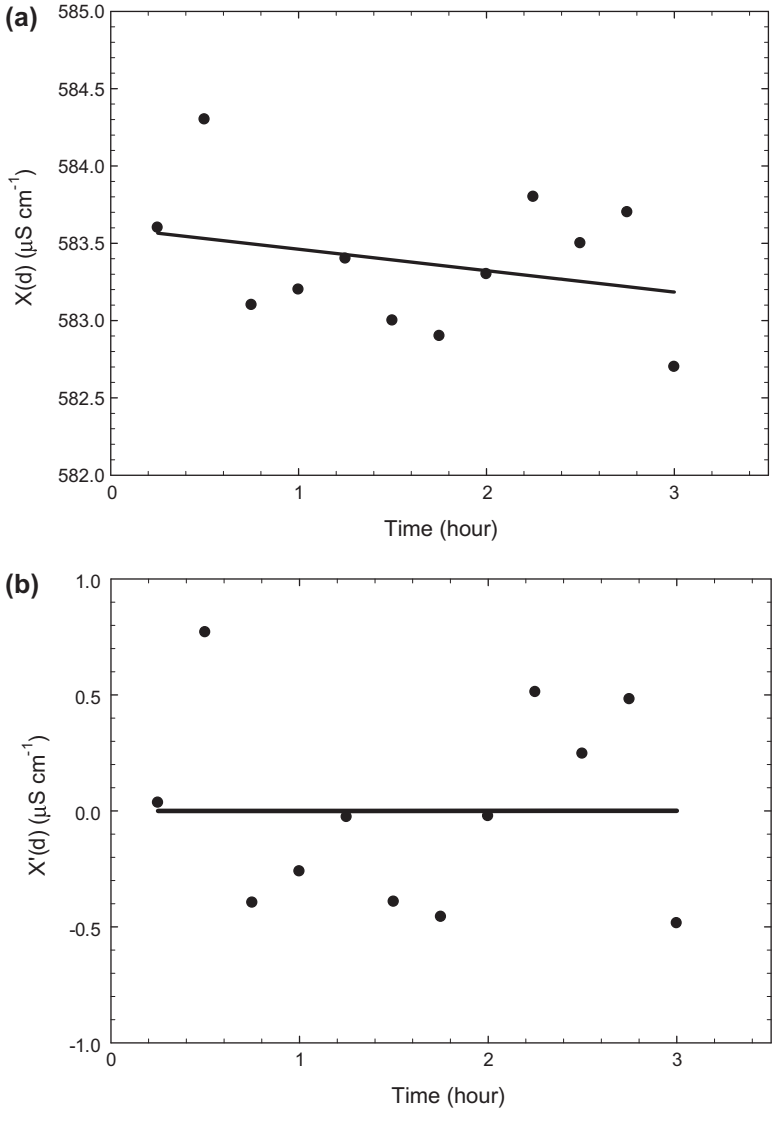

Figure 2. (a) Raw and (b) detrended $EC_{25°C}$ data from time block 1 of the HOBO sensor at GC01 for deployment 3.

The variable τ is the lag coefficient, which in this case is 1 because a lag of one period (e.g. 3-h time block) was used.

Following computation of the white noise for each $EC_{25°C}$ data point, the variance of the white noise for each 3-h time block was computed using Equation (4).

$$S^2(t) = \frac{1}{n-1}\sum_{i=1}^{n}[a(d)_i - \overline{a(d)}]^2 \tag{4}$$

The variable S^2 is the variance of the white noise for the 3-h time block (μS^2 cm^{-2}); n is the number of data points within that time block; and $\overline{a(d)}$ is the mean value of $EC_{25°C}$ (μS cm^{-1}).

Prior to comparison with the variance of the white noise for each time block, all three variables (white noise variance, $EC_{25°C}$, and discharge) required transformation using Equations (5)–(7) to remove autocorrelation.

$$X^*_{i,d} = X_{i,d} - \rho X_{i,d-1} \tag{5}$$

$$Y^*_{i,d} = Y_{i,d} - \rho Y_{i,d-1} \tag{6}$$

$$Z^*_{i,d} = Z_{i,d} - \rho Z_{i,d-1} \tag{7}$$

The variable X^* is the transformed $EC_{25°C}$ data (μS cm^{-1}); Y^* is the transformed discharge data (m^3 s^{-1}); Z^* is the transformed white noise variance (μS^2 cm^{-2}). Following transformation, the respective data were averaged to determine a mean transformed $EC_{25°C}$ and transformed discharge for each time block.

Statistical analysis

An analysis of covariance (ANCOVA) was used to compare differences in white noise variance between all four sensors at each location and all three locations within each sensor type [32,33]. The covariates were sensor type and location adjusted for deployment period. Multiple linear regression models were used to determine the effects of transformed $EC_{25°C}$ (X^*) and transformed discharge (Y^*) on transformed white noise variance (Z^*) (Systat Software, Inc.). Each variable (X^*, Y^* and Z^*) was transformed to normalise the data. Since the detrended data had both positive and negative values, the data were squared before applying a natural log transformation [33]. In all instances, a significance level of $p = 0.05$ was used.

Results and discussion

Study site comparisons

Tables 4 and 5 contain non-detrended and non-transformed white noise variance and $EC_{25°C}$ means and standard errors for each sensor, deployment and location combination. Both white noise variance and $EC_{25°C}$ were smallest at LMS and highest at GC03. White noise variance at LMS was typically less than 2 μS^2 cm^{-2}, across all sensors; similarly, $EC_{25°C}$ was generally less than 80 μS cm^{-1} for the study period. Values for white noise variance were highest with the HOBO sensors as were $EC_{25°C}$ values. In a

Table 4. Mean (*M*) and standard errors (SE) of non-detrended and non-transformed white noise variance ($\mu S^2\ cm^{-2}$).

	Location		
Sensor/deployment[a]	LMS	GC01	GC03
YSI			
1	0.4 ± 0.1	0.7 ± 0.1	2127.5 ± 211.5
2	3.1 ± 1.2	–	1911.8 ± 799.7
3	0.2 ± 0.1	–	2398.3 ± 1644.2
4	0.4 ± 0.1	8.4 ± 5.1	1206.5 ± 524.1
5	–	–	–
6	0.4 ± 0.2	–	–
7	–	2.5 ± 0.4	776.7 ± 371.7
M ± SE	1.0 ± 0.3	4.1 ± 1.7	1560.5 ± 310.4
HOBO			
1	0.1 ± 0.0	0.4 ± 0.1	13.9 ± 9.1
2	1.3 ± 0.7	51.5 ± 18.7	9091.1 ± 2016.7
3	0.1 ± 0.0	31.6 ± 17.7	1478.1 ± 1058.6
4	0.3 ± 0.1	18.1 ± 155.6	546.7 ± 265.0
5	8.4 ± 2.2	1.5 ± 0.6	46.6 ± 22.9
6	0.3 ± 0.1	2.9 ± 0.1	5.4 ± 1.5
7	1.2 ± 0.9	6.2 ± 32.4	13.9 ± 9.1
M ± SE	1.7 ± 0.4	14.8 ± 113.7	1586.2 ± 333.3
Solinst			
1	–	–	–
2	–	–	–
3	–	–	–
4	0.2 ± 0.1	2.5 ± 1.5	48,218.5 ± 14,387.6
5	1.9 ± 0.4	0.3 ± .01	81,033.5 ± 14,089.9
6	0.5 ± 0.1	0.9 ± 0.4	34,585.2 ± 5533.4
7	–	1.1 ± 0.6	21,659.1 ± 2825.9
M ± SE	0.8 ± 0.1	1.2 ± 0.4	44,323.1 ± 4819.1
Aqua TROLL			
1	–	–	–
2	–	–	–
3	–	–	–
4	0.2 ± 0.1	14.2 ± 4.5	72,608.7 ± 34,209.8
5	0.3 ± 0.1	0.1 ± 0.0	11.9 ± 3.6
6	0.3 ± 0.1	0.4 ± 0.2	94.8 ± 66.7
7	0.1 ± 0.0	0.3 ± 0.3	277.6 ± 205.3
M ± SE	0.2 ± 0.1	3.3 ± 1.1	16,036.8 ± 7571.9

[a]Deployment periods: 1 = 16 March 2011–1 April 2011 (17 days); 2 = 14 April 2011–5 May 2011 (22 days); 3 = 19 May 2011–29 May 2011 (11 days); 4 = 23 June 2011–13 July 2011 (21 days); 5 = 28 July 2011–17 August 2011 (21 days); 6 = 8 September 2011–6 October 2011 (29 days) for HOBO, Solinst and Aqua Troll and 8 September 2011–28 September 2011 (21 days) for YSI; and 7 = 28 October 2011–20 November 2011 (23 days) for HOBO, Solinst and Aqua Troll and 28 October 2011–17 November 2011 (21 days) for YSI.

laboratory study, Maupin et al. [21] found that the HOBO sensors tended to over-estimate $EC_{25°C}$ (5–9986 μS cm^{-1} range), which may be the case here as well. At GC01, white noise variance was also highest with the HOBO sensors; however, $EC_{25°C}$ values were similar to those of the other sensors. White noise variance values were generally low, like at LMS, with the exception of the HOBO sensors which posted values from about 1 $\mu S^2\ cm^{-2}$ up to about 50 $\mu S^2\ cm^{-2}$. At GC03, both white noise variance and $EC_{25°C}$ increased substantially. White noise variance was highest with the Solinst

Table 5. Mean (*M*) and standard errors (SE) of non-detrended and non-transformed $EC_{25°C}$ (μS cm^{-1}).

	Location		
Sensor/deployment[a]	LMS	GC01	GC03
YSI			
1	42.8 ± 0.2	301.4 ± 1.4	1930.1 ± 3.8
2	39.4 ± 0.4	–	1571.3 ± 25.9
3	41.1 ± 0.1	–	2069.1 ± 21.1
4	58.1 ± 0.3	570.1 ± 2.1	2338.6 ± 15.3
5	–	–	–
6	67.1 ± 1.0	–	–
7	–	498.3 ± 14.1	2325.3 ± 34.7
M ± SE	50.9 ± 0.5	485.9 ± 7.9	2057.7 ± 16.6
HOBO			
1	66.8 ± 1.4	462.5 ± 5.8	2129.0 ± 2.8
2	91.9 ± 2.3	279.8 ± 91.2	1584.6 ± 26.7
3	137.8 ± 1.2	546.4 ± 3.7	2151.3 ± 21.9
4	76.4 ± 0.3	705.4 ± 5.3	2384.3 ± 10.8
5	54.3 ± 1.2	1099.2 ± 19.0	2397.2 ± 3.1
6	70.8 ± 6.1	654.3 ± 1.2	2457.1 ± 5.5
7	65.9 ± 1.2	530.8 ± 6.4	2129.0 ± 2.8
M ± SE	75.7 ± 0.8	627.7 ± 8.4	2200.6 ± 10.4
Solinst			
1	–	–	–
2	–	–	–
3	–	–	–
4	45.6 ± 0.3	656.1 ± 5.6	2457.4 ± 55.6
5	52.7 ± 1.0	674.5 ± 3.7	3618.9 ± 47.2
6	62.0 ± 0.8	644.9 ± 1.6	2492.5 ± 36.6
7	–	552.6 ± 5.8	2817.0 ± 63.7
M ± SE	54.4 ± 0.5	629.9 ± 2.8	2814.1 ± 30.5
Aqua TROLL			
1	–	–	–
2	–	–	–
3	–	–	–
4	61.1 ± 0.6	539.3 ± 4.4	2261.1 ± 34.8
5	77.5 ± 1.0	462.1 ± 2.2	2264.3 ± 3.3
6	70.8 ± 0.4	668.8 ± 1.5	2245.2 ± 10.6
7	80.3 ± 1.8	665.7 ± 1.7	2101.2 ± 28.3
M ± SE	72.6 ± 0.6	594.8 ± 3.5	2215.6 ± 11.3

[a]Deployment periods: 1 = 16 March 2011–1 April 2011 (17 days); 2 = 14 April 2011–5 May 2011 (22 days); 3 = 19 May 2011–29 May 2011 (11 days); 4 = 23 June 2011–13 July 2011 (21 days); 5 = 28 July 2011–17 August 2011 (21 days); 6 = 8 September 2011–6 October 2011 (29 days) for HOBO, Solinst and Aqua Troll and 8 September 2011–28 September 2011 (21 days) for YSI; and 7 = 28 October 2011–20 November 2011 (23 days) for HOBO, Solinst and Aqua Troll and 28 October 2011–17 November 2011 (21 days) for YSI.

sensors averaging over 44,000 μS^2 cm^{-2} across the four deployment periods it was in use. The Aqua TROLL has the next highest white noise variance values with a mean of around 16,000 μS^2 cm^{-2}. Both the YSI and HOBO sensors have similar white noise variance means with values of around 1500 μS^2 cm^{-2}. Mean $EC_{25°C}$ varied much less between sensors with values ranging from about 2050 to 2800 μS cm^{-1}.

Table 6 contains the non-detrended and non-transformed discharge means and standard errors for each deployment and location combination. Mean discharge was lowest

Table 6. Mean (M) and standard errors (SE) of non-detrended and non-transformed discharge ($m^3\ s^{-1} \times 10^{-3}$).

	Location		
Deployment[a]	LMS	GC01	GC03
1	17.3 ± 0.3	2.5 ± 0.7	3.8 ± 0.1
2	90.5 ± 11.3	2.8 ± 0.1	17.7 ± 1.4
3	75.7 ± 12.5	1.2 ± 0.1	5.5 ± 0.2
4	12.2 ± 2.9	1.7 ± 0.0	2.7 ± 0.2
5	25.2 ± 4.4	1.6 ± 0.0	2.6 ± 0.0
6	3.7 ± 0.6	1.4 ± 0.0	2.1 ± 0.0
7	8.9 ± 1.0	1.3 ± 0.0	2.4 ± 0.1
M ± SE	28.1 ± 2.2	1.8 ± 0.0	5.1 ± 0.3

[a]Deployment periods: 1 = 16 March 2011–1 April 2011 (17 days); 2 = 14 April 2011–5 May 2011 (22 days); 3 = 19 May 2011–29 May 2011 (11 days); 4 = 23 June 2011–13 July 2011 (21 days); 5 = 28 July 2011–17 August 2011 (21 days); 6 = 8 September 2011–6 October 2011 (29 days) for HOBO, Solinst and Aqua Troll and 8 September 2011–28 September 2011 (21 days) for YSI; and 7 = 28 October 2011–20 November 2011 (23 days) for HOBO, Solinst and Aqua Troll and 28 October 2011–17 November 2011 (21 days) for YSI.

at GC01 (0.1 $m^3\ s^{-1}$) followed by GC03 (0.2 $m^3\ s^{-1}$) and then LMS (1.0 $m^3\ s^{-1}$). This order does not correspond to white noise variance and $EC_{25°C}$ values which increased in the order of LMS, GC01 and then GC03. Mean discharges were higher during deployments 2 and 3 which together encompassed mid-April through May of 2011.

Figures 3–5 show $EC_{25°C}$ measurements for all four sensor types at LMS, GC01 and GC03, respectively. Figure 4 shows all three locations during the same deployment period. At LMS, all four sensors recorded similar $EC_{25°C}$ values. The Solinst recorded $EC_{25°C}$ values about 20 μS cm^{-1} lower than the other sensors at the beginning of deployment period 6 while the Aqua TROLL recorded values about 20 μS cm^{-1} greater

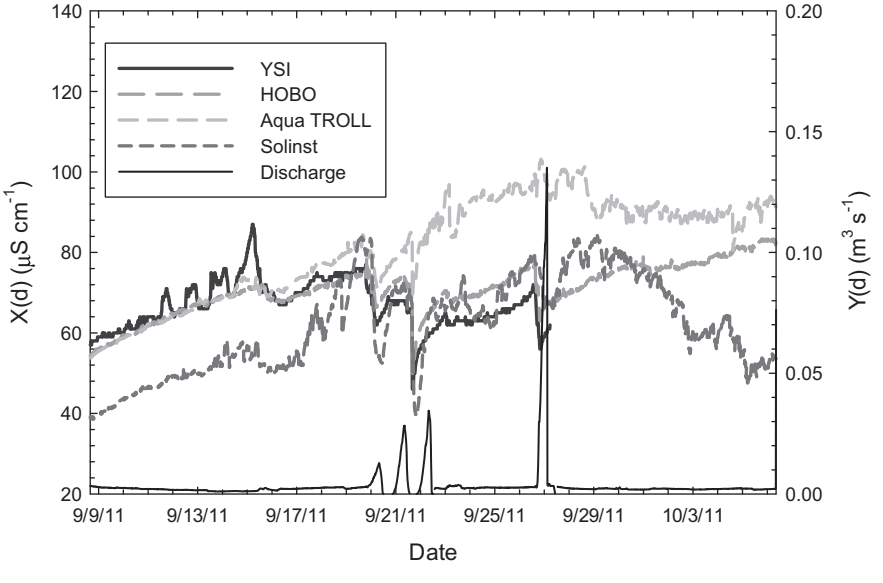

Figure 3. $EC_{25°C}$ readings and discharge at LMS during deployment 6.

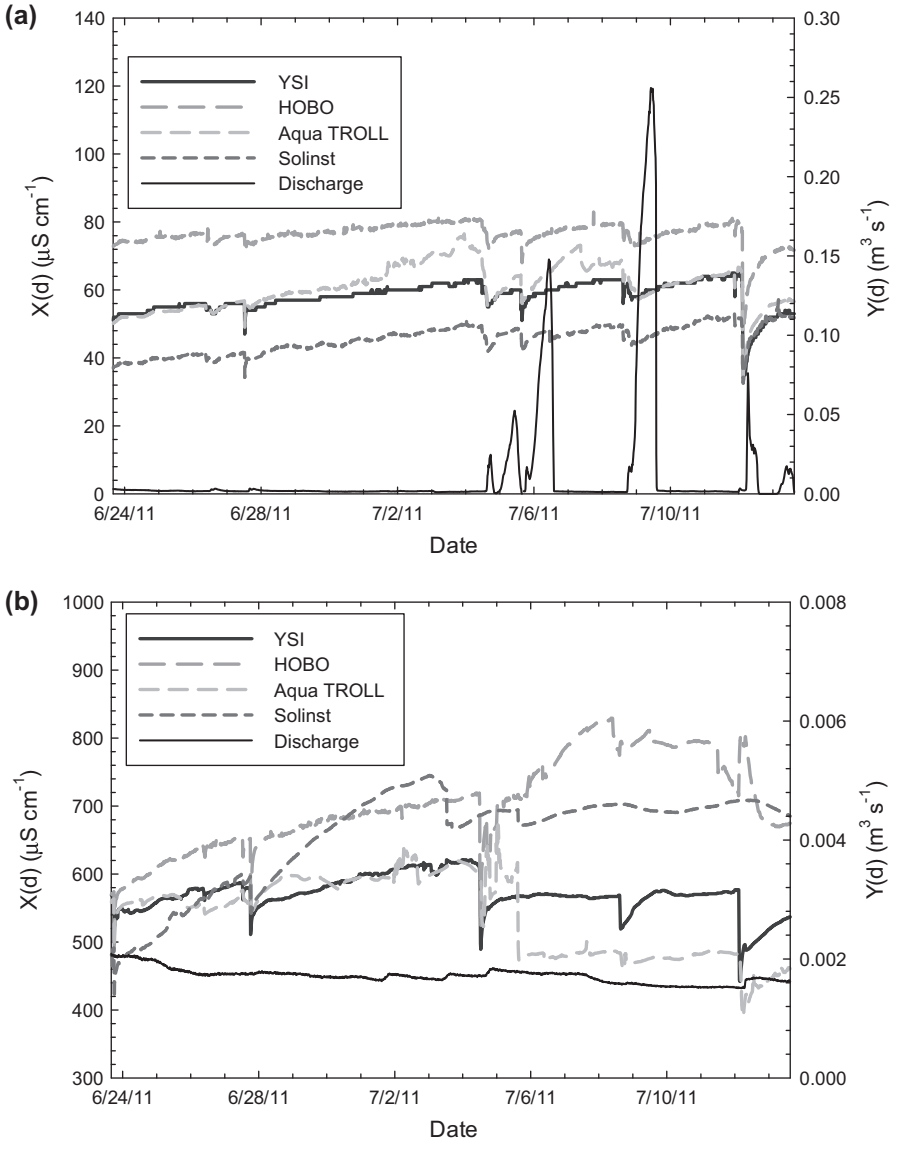

Figure 4. $EC_{25°C}$ readings and discharge during deployment 4 at (a) LMS, (b) GC01 and (c) GC03.

than the others for the latter part of this deployment period (Figure 3). The reason for this shift is not known. No appreciable rainfall events, those greater than 12.5 mm, occurred during this deployment period. During deployment period 4, the Solinst also recorded lower $EC_{25°C}$ values as compared to the other sensors. The Aqua TROLL and YSI recorded similar $EC_{25°C}$ values during this period while the HOBO recorded the highest $EC_{25°C}$ values (Figure 4(a)). Precipitation events during deployment period 4 caused $EC_{25°C}$ values to drop slightly at LMS.

At GC01, where $EC_{25°C}$ is higher as compared to LMS, the pattern of which sensor typically recorded the highest and lowest $EC_{25°C}$ values different (Figure 4(b)). While

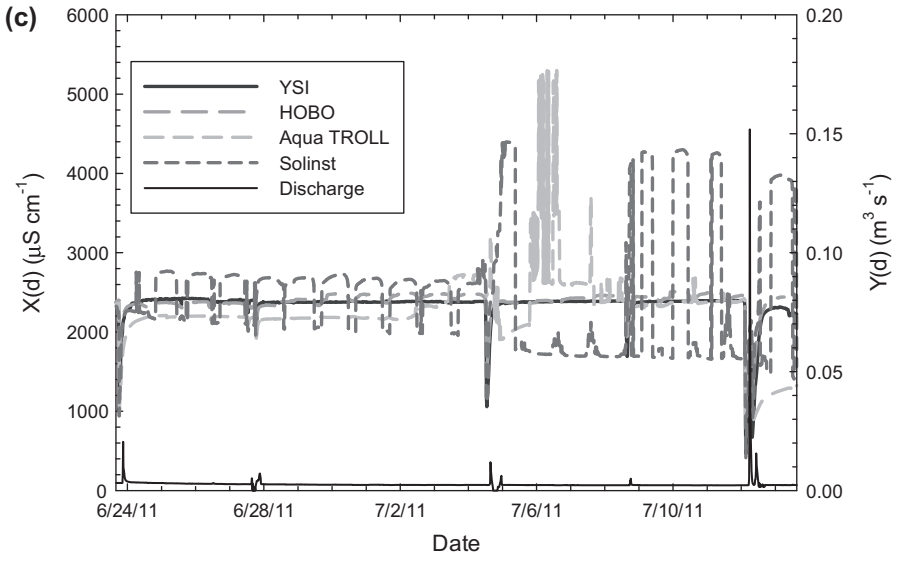

Figure 4. (*Continued*).

the HOBO consistently records higher $EC_{25°C}$ values than the other sensors, the Aqua TROLL largely records lower $EC_{25°C}$ values. The Solinst has a large increase in $EC_{25°C}$ around June 28, 2011 although no rain events, and hence no change in discharge, were recorded at that time. $EC_{25°C}$ readings from the YSI were fairly constant across the period. Table 4 shows that the white noise variance for the sensors at GC01 was comparable to LMS with the exception of the HOBO sensor which recorded the highest variances in addition to the highest $EC_{25°C}$ values. Two rain events greater than 12.5 mm occurred during this deployment period: 19.3 mm on 11 July 2011 and 14.2 mm on 14 July 2011. However, no rain events were recorded at GC01 between 4 July 2011 and 6 July 2011 when the Aqua TROLL $EC_{25°C}$ readings fluctuated largely. A daily rainfall amount of 1 mm was recorded at the nearest NOAA weather station in Jackson, Kentucky which is about 20 km from Robinson Forest. The reason for this fluctuation is not known, but the YSI and HOBO sensors also dipped at this time while the Solinst did not. It is possible that an isolated rain event occurred that was not recorded by the onsite weather station or the NOAA weather station in Jackson, Kentucky.

The $EC_{25°C}$ readings at GC03 showed large variations, particularly with regards to the Solinst sensor (Figures 4(c) and 5). This sensor displayed large fluctuations that resembled a diurnal pattern. This cyclic pattern was not seen in any of the other sensors. Even though temperature corrected conductivity values were used, a check of the temperature data from all sensors at this site did not reveal any notable temperature fluctuations that would have accounted for the cyclical pattern with the Solinst. The Solinst sensors used at LMS and GC01 were deployed at GC03 for an eight-day period in December 2012. Like the Solinst output at GC03, as seen in Figures 5(c) and 6, the $EC_{25°C}$ values from these sensors also displayed a cyclic pattern indicating that the cause is likely due in part to sensor construction. The Solinst sensor has a relatively large open conductivity cell in which four bars span the width of the cell. Following examination of the results from the other two Solinst sensors at GC03, consultation

with the manufacturer revealed that a biofoul screen is likely needed when using this sensor in iron-precipitate-laden waters such as those present at GC03.

As with GC01, the HOBO sensor recorded the highest $EC_{25°C}$ values during deployment period 7. HOBO $EC_{25°C}$ values at GC03 were about 250 μS cm^{-1}–1000 μS cm^{-1} higher than those recorded by the YSI and Aqua TROLL sensors. Grab samples collected at the start and end of the deployment period 7, which were analysed for $EC_{25°C}$ using a YSI Model 35 (YSI Incorporated, Yellow Springs, OH, USA) in the University of Kentucky Forestry Department, were 2020 and 1582 μS cm^{-1}, respectively. As seen in Figure 5, these laboratory measured values were close to the starting and ending values of the HOBO sensor at GC03, which were 2413 and 1550 μS cm^{-1}, respectively. The other sensors measured considerably lower $EC_{25°C}$ values at the start of the deployment period, as compared to the grab sample, but were more similar at the end of the deployment period. No grab samples were collected during the deployment period to which comparisons can be made. For deployment period 4, as seen in Figure 4 (c), the HOBO sensor recorded $EC_{25°C}$ values quite comparable to the YSI and the Aqua TROLL, with the exception of a two-day period when the Aqua TROLL recorded an erratic pattern of data. The reason for this sudden increase in $EC_{25°C}$ values followed by a rapid decrease is not known. This pattern did not appear again during any of the deployment periods. Two rain events occurred during deployment period 7: 15.5 mm on 2 November 2011 and 29.2 mm on 5 November 2011. All four sensors noted the drop in $EC_{25°C}$ values associated with the dilution effect of the run-off.

As seen in Table 4, white noise variance was highest at GC03 with white noise variances in the 1000s or even 10,000s with the Solinst sensor. Based on work by Maupin et al. [21], it was expected that the sensors would display temporal stability at the expected $EC_{25°C}$ values at GC03, based on work by Fritz et al. [22]. These $EC_{25°C}$ values were much less than the maximum of 9986 μS cm^{-1} used in the study. And even at that level, all sensors displayed temporal stability, in the laboratory study by Maupin et al. [21] at water temperatures encountered at the sites (10–15 °C) with the exception of the HOBO sensors.

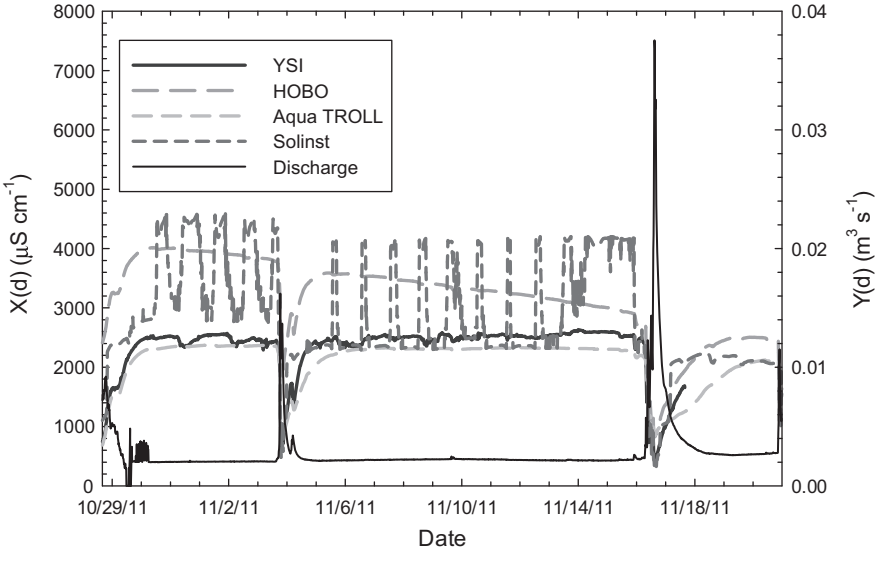

Figure 5. $EC_{25°C}$ readings and discharge at GC03 during deployment 7.

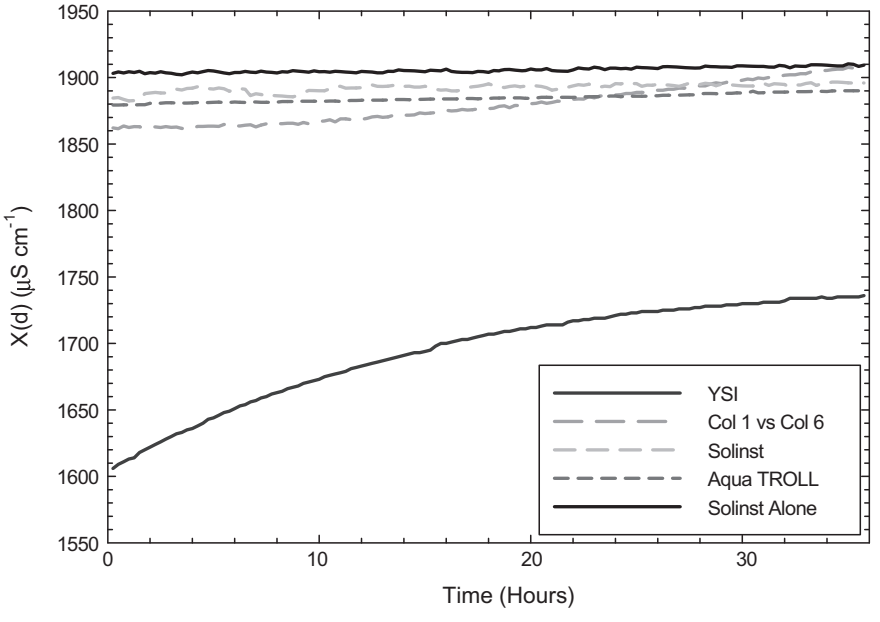

Figure 6. Results of laboratory signal interference testing in water from GC03.

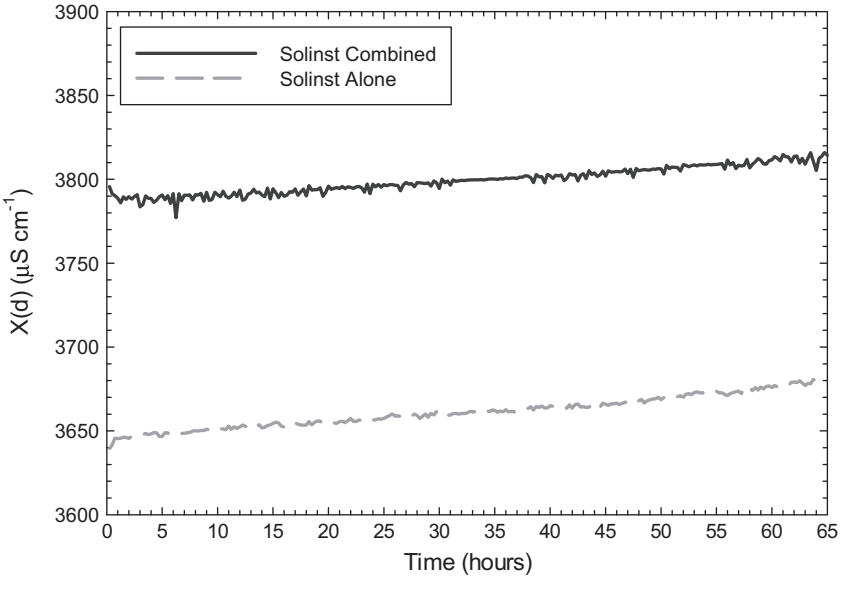

Figure 7. Results of laboratory signal interference testing in $EC_{25°C}$ standard solution. *Solinst combined indicates presence of YSI, HOBO and Aqua TROLL sensors with Solinst sensor.*

The temporal variability seen at GC03, in light of the results from the laboratory experiments carried out by Maupin et al. [21], suggests that a constituent or combination of constituents in the water was negatively affecting the performance of the sensors, particularly the Solinst sensor. Mastin et al. [34] noted that the mixed

Table 7. Means (*M*) and standard errors (SE) of detrended and transformed white noise variance for sensor type and location for all deployment periods.[a]

	Location		
Sensor	LMS	GC01	GC03
YSI	−1.6 ± 0.3 a,y[b]	−1.4 ± 0.3 a,y	4.6 ± 0.2 b,x
HOBO	−2.2 ± 0.2 b,z	−1.4 ± 0.2 a,y	0.4 ± 0.2 c,x
Aqua TROLL	−5.0 ± 0.2 c,y	−6.7 ± 0.2 c,z	−0.8 ± 0.2 d,x
Solinst	−2.5 ± 0.3 b,z	−4.1 ± 0.2 b,y	6.3 ± 0.2 a,x

[a]Larger values indicate greater levels of white noise.
[b]For each constituent, within-column means followed by the same letter (a, b, c or d) are not significantly different ($\alpha = 0.05$). For each constituent, within-row means followed by the same letter (x, y or z) are not significantly different ($\alpha = 0.05$).

Table 8. Coefficients and intercepts of $EC_{25°C}$ and discharge versus white noise variance for each sensor type.

Variable[a]	Coefficient	Standard error	*p*-value	R^2
YSI				
$EC_{25°C}$	1.29	0.04	<0.001	0.47
Discharge	0.05	0.02	0.039	
HOBO				
$EC_{25°C}$	1.03	0.02	<0.001	0.39
Discharge	0.06	0.02	<0.001	
Solinst				
$EC_{25°C}$	1.72	0.03	<0.001	0.65
Discharge	0.08	0.03	0.007	
Aqua TROLL				
$EC_{25°C}$	1.20	0.04	<0.001	0.35
Discharge	0.10	0.03	<0.001	

[a]Detrended and transformed.

chemistry of the mine drainage emitted from the toe of the valley fill was impacting a bioreactor treatment system installed at the site. The authors measured low iron levels (<4 mg L^{-1}) in the mine drainage emitted from the toe of the valley fill at Guy Cove, which is in close proximity to GC03. However, these levels were sufficient to precipitate in surface waters due to oxygen exposure, thus clogging plumbing to passive treatment bioreactors. The GC03 site is the only one of the three studied with an orange, iron-precipitate-laden biofilm present on the streambed. Whelan and Regan [9] noted a biofilm can begin to form on sensors quite quickly (e.g. minutes) after immersion in water, and that this biofilm negatively affects sensor performance. To minimise the impacts of fouling, each sensor was cleaned at the end of all deployment periods. Regardless, some discolouration did occur on the sensor housings. In the case of the Solinst sensor, likely due to the way in which the conductivity cell is constructed, a biofoul screen is recommended before using this sensor in waters such as those at GC03.

White noise variance evaluation

Results from the ANCOVA analysis showed that, in most instances, each sensor produced a significantly different level of white noise variance for each location. At

LMS, the Aqua TROLL had the lowest level of white noise variance while the YSI had the highest (Table 7). The HOBO and Solinst did not differ at LMS. A similar trend was observed at GC01 and GC03 with the Aqua TROLL recording significantly less white noise variance than the other sensors. At GC01, the YSI and the HOBO had the highest level of white noise variance while at GC03 the Solinst recorded a much greater level of white noise variance than the other sensors. A comparison of sensor performance between locations revealed that for all sensor types the largest amount of white noise variance occurred at GC03 followed predominately by GC01 and then LMS. While each of these sites has different average $EC_{25°C}$ values, as seen in Table 1, the sites also have different average discharges as noted in Table 6. Discharges are typically largest at LMS followed by GC03 and then GC01.

Results from the multiple linear regression analyses show that white noise variance was significantly related to $EC_{25°C}$ and discharge for all of the sensors (Table 8). For the YSI sensors, results of the regression analysis indicated that the model was able to explain 47% of the white noise variance ($R^2 = 0.47$). For the HOBO sensors, the R^2 was 0.39; $R^2 = 0.65$ for the Solinst; and $R^2 = 0.35$ for the Aqua TROLL. An increase in $EC_{25°C}$ and discharge resulted in an increase in the white noise variance for all sensor types. However, with the exception of the Solinst sensor, all of the other sensors were comparable in the effect of $EC_{25°C}$ and discharge on sensor performance. Increases in $EC_{25°C}$ had the largest influence on the Solinst sensors followed by the YSI, Aqua TROLL and HOBO. A 1% increase in $EC_{25°C}$ produces a 1.7% increase in white noise variance for the Solinst sensors. For the YSI, Aqua TROLL and HOBO sensors, a 1% increase in $EC_{25°C}$ results in a 1.3, 1.2 and 1% increase, respectively, in white noise variance. These results indicate that as $EC_{25°C}$ levels increase, the noise present in the sensor readings increases as well, particularly for the Solinst sensor. These findings suggest that one avoids using the Solinst sensor in waters such as those at GC03.

Increases in discharge had a much smaller effect on white noise variance. A 1% increase in discharge produced a 0.1% or less increase in white noise variance for all sensors. While significant, these results indicate that discharge has little effect on white noise variance. This result was somewhat expected as the conductivity sensors are not measuring discharge. Rather, changes in discharge affect $EC_{25°C}$ values. As discharge increases, as seen in Figures 3–5, $EC_{25°C}$ values tend to decrease due to the diluting effect of the run-off. These results indicate that shifts in discharge, such as with storm events, have minimal impacts on white noise variance. Thus, it is expected that these sensors will perform comparably well under a wide range of discharges, even those that change rapidly. These findings indicate that the hydrology of a site (e.g. discharge volume, time to peak, etc.) is not an important consideration in conductivity sensor selection.

Signal interference

Based on unexpected cyclic nature of the Solinst $EC_{25°C}$ readings, the possibility of signal interference between the conductivity sensors was investigated using waters collected from GC03 as well as a standard $EC_{25°C}$ solution of 3860 μS cm^{-1}. Using a hose connected to a PVC pipe with multiple 3.2 mm holes, compressed air was bubbled through both solutions to prevent settling and to simulate water movement in a stream riffle as all sensors were placed in riffles in the field. In the first trial, one sensor each from all four sensor types was simultaneously placed into the GC03 collected waters. These sensors were the same four sensors deployed at GC03. Data were collected at 15-min intervals, as was done in the field, for over a 24-h period. The trial was repeated

for a YSI-supplied standard calibration solution ($EC_{25°C} = 3860$ μS cm^{-1}). A second trial was also conducted in the same manner using only the Solinst sensor (i.e. only one sensor in the container).

In the GC03 waters and the standard YSI calibration solution, the Solinst sensor performed in a similar manner whether grouped with the other sensors or alone (Figures 6 and 7). No cyclic patterns were observed. Hence, signal interference from other sensors is not an issue. The lack of cyclic patterns in the Solinst sensor output when tested in GC03 waters during this laboratory study suggests that sensor fouling in the field is the likely the cause of the erratic readings. In the field, a thick layer of iron precipitate is present on top of the streambed at GC03. Such precipitates were not present in the laboratory study.

Conclusions

Four commonly used $EC_{25°C}$ sensors (YSI, HOBO, Solinst and Aqua TROLL) were evaluated at three study sites located on forested and mined lands in eastern Kentucky. Water quality at the sites varied with typical $EC_{25°C}$ values from grab samples of about 40, 450 and 1700 μS cm^{-1} at LMS, GC01 and GC03, respectively. Seven deployment periods spanning the months of March through November of 2011, for a total of about 135 days, were evaluated. For each sensor at each site, white noise variance was computed and compared to $EC_{25°C}$ and discharge. An ANCOVA was used to compare sensor performance at each location and across locations. For all sensor types, the largest amount of white noise variance was associated with GC03 followed by GC01 and then LMS. At each location, white noise variance differed significantly between all sensors though the biggest difference was noted with the Solinst at GC03. Multiple linear regression analysis was used to assess the strength of the relationship between $EC_{25°C}$, discharge and white noise variance. Results from the ANCOVA analysis indicated that all sensors performed differently at each location and across locations. Results from the multiple regression analyses indicate that the model explains 65% of the white noise variance with the Solinst sensors, 47% for YSI sensors, 39% for HOBO sensors, and 35% for Aqua TROLL sensors.

While both independent variables were significant predictors of white noise variance, increases in $EC_{25°C}$ had a much larger effect than increases in discharge. The small effect of discharge on white noise variance indicates that changes in discharge, as in the case of storm events, have minimal impact on sensor performance. As the sensors do not directly measure discharge, this small effect is likely attributable to the dilution effect of increased stream flows resulting from run-off on $EC_{25°C}$ values.

Of greater concern is that the Solinst sensors consistently displayed a cyclic pattern at GC03, the site with the highest $EC_{25°C}$ levels. Laboratory tests using waters collected from GC03 as well as a diluted standard $EC_{25°C}$ solution eliminated the possibility of signal interference from the other sensors. Deployment of the Solinst sensors used at LMS and GC01 during December 2012 showed that those sensors also displayed a cyclic pattern. Based on an evaluation of the Solinst sensor construction, it is suspected that fouling at GC03 caused the Solinst sensors to report widely fluctuating $EC_{25°C}$ values. Iron precipitates are prevalent at GC03. Further investigation with the manufacturer revealed that a biofoul screen is likely needed when using the Solinst in the conditions present at GC03.

Conductivity sensor selection can be a challenging task, particularly when monitoring waters emanating from mined lands as well as sites impacted by oil and gas

extraction. The mixed chemistry in the waters at these sites means that sensor ruggedness becomes a critical factor. Even with regular cleaning and calibration, sensor fouling can occur rapidly, within hours or days, in locations where precipitates are common, such as at the toe of a valley fill. Lastly, consideration should be given to the small sample size. Due to budgetary limitations, only one sensor of each type could be tested at each site. It is possible that a different sensor, of the same sensor type, would perform differently.

Acknowledgements

The authors would like to thank Kristen McQuerry for her statistical assistance as well as Emma Witt and Matt Strong for their assistance in collecting the data. This project was funded by the Kentucky Department of Fish and Wildlife Resources (PON2 660 1000003368 1), Virginia Tech University and the ARIES Program (441693-19660A). Any opinions, findings and conclusions or recommendations expressed in this publication are those of the authors and do not necessarily reflect the views of the Kentucky Department of Fish and Wildlife Resources, Virginia Tech University or the ARIES Program. Mention of trade names or commercial products does not constitute endorsement or recommendation for use.

References

[1] D. Kobayashi, K. Suzuki, and M. Nomura, *Diurnal fluctuations in stream flow and in specific electric conductance during drought periods*, J. Hydrol. 115 (1990), pp. 105–114.

[2] A.W. Fogle, J.L. Taraba, and J.S. Dinger, *Mass load estimation errors utilizing grab sampling strategies in a karst watershed*, JAWRA, 39 (2003), pp. 1361–1372.

[3] D.S. Ahern, R.W. Sheibley, and R.A. Dahlgren, *Effects of river regulation on water quality in the Lower Mokelumne River California*, River Res. Appl. 21 (2005), pp. 651–670.

[4] G.J. Pond, M.E. Passmore, F.A. Borsuk, L. Reynolds, and C.J. Rose, *Downstream effects of mountaintop coal mining: Comparing biological conditions using family- and genus-level macroinvertebrate bioassessment tools*, J. N. Am. Benthol. Soc. 27 (2008), pp. 717–737.

[5] R.J. Wagner, H.C. Mattraw, G.F. Ritz, and B.A. *Smith. Guidelines and standard procedures for continuous water-quality monitors: Site selection, field operation, calibration, record computation, and reporting*. Techniques and Methods 1–D3. U.S. Geological Survey, Reston, VA, 2006.

[6] M.B. Henjum, R.M. Hozalski, C.R. Wennen, W. Arnold, and P.J. Novak, *Correlations between in situ sensor measurements and trace organic pollutants in urban streams*, J. Environ. Monitor. 12 (2010), pp. 225–233.

[7] M.S. Tomlinson and E.H. De Carlo, *The need for high resolution time series data to characterize Hawaiian streams*, JAWRA, 39 (2003), pp. 113–123.

[8] J.W. Kirchner, X. Feng, C. Neal, and A.J. Robson, *The fine structure of water-quality dynamics: The* (*high-frequency*) *wave of the future*, Hydrol. Process. 18 (2004), pp. 1353–1359.

[9] A. Whelan and F. Regan, *Antifouling strategies for marine and riverine sensors*, J. Environ. Monitor. 8 (2006), pp. 880–886.

[10] N.S. Miguntanna, P. Egodawatta, S. Kokot, and A. Goonetilleke, *Determination of a set of surrogate parameters to assess urban stormwater quality*, Sci. Total Environ. 408(2010) (2010), pp. 6251–6259.

[11] A.S. Jones, D.K. Stevens, J.S. Horsburgh, and N.O. Mesner, *Surrogate measures for providing high frequency estimates of total suspended solids and total phosphorus concentrations*, JAWRA, 47 (2011), pp. 239–253.

[12] T.N. Williamson and C.G. Crawford, *Estimation of suspended-sediment concentration from total suspended solids and turbidity data for Kentucky, 1978–1955*, JAWRA, 47 (2011), pp. 739–749.

[13] A.P. Stubblefield, J.E. Reuter, R.A. Dahlgren, and C.R. Goldman, *Use of turbidometry to characterize suspended sediment and phosphorus fluxes in the Lake Tahoe basin, California, USA*, Hydrol. Process. 21(2007) (2007), pp. 281–291.
[14] G. Tchobanoglous, F.L. Burton, and H.D. Stensel, *Wastewater Engineering: Treatment and Use*, 4th ed. ed., McGraw-Hill, New York, NY, 2003.
[15] S. Settle, A. Goonetilleke, and G. Ayoko, *Determination of surrogate indicators for phosphorus and solids in urban stormwater: Application of multivariate data analysis techniques*, Water Air Soil Poll. 182(2007) (2007), pp. 149–161.
[16] G.J. Pond, *Biodiversity loss in Appalachian headwater streams (Kentucky, USA): Plecoptera and Trichoptera communities*, Hydrobiologia, 679 (2012), pp. 97–117.
[17] G.J. Pond, *Patterns of Ephemeroptera taxa loss in Appalachian headwater streams (Kentucky, USA)*, Hydrobiologia, 641(2010) (2010), pp. 185–201.
[18] T.T. Lindberg, E.S. Bernhardt, R. Bier, A.M. Helton, R.B. Merola, A. Vengosh, and R.T. Di Giulo, *Cumulative impacts of mountaintop mining on an Appalachian watershed*, Proc. Natl Acad. Sci. USA, 108 (2011), pp. 20929–20934.
[19] E.R. Merriam, J.T. Petty, G.T. Merovich, Jr., J.B. Fulton, and M.P. Strager, *Additive effects of mining and residential development on stream conditions in a central Appalachian watershed*, J. N. Am. Benthol. Soc. 30 (2011), pp. 399–418.
[20] United States Environmental Protection Agency, *Memorandum, improving EPA review of appalachian surface coal mining operations under the Clean Water Act, National Environmental Policy Act, and the Environmental Justice Executive Order*, 2011. Available at: http://water.epa.goc/owow/wetlands/guidance/pdf/appalachia_mtntop_mining_summary.pdf.
[21] T.P. Maupin, C.T. Agouridis, C.D. Barton, R.C. Warner, and X. Yu. *Specific conductivity sensor performance. I Laboratory evaluation*. Int. J. Mini. Reclamat. Environ., in this issue.
[22] K.M. Fritz, S. Fulton, B.R. Johnson, C.D. Barton, J.D. Jack, D.A. Word, and R.A. Burke, *Structural and functional characteristics of natural and constructed channels draining a reclaimed mountaintop removal and valley fill coal mine*, J.N. Am. Benthol. Soc. 29 (2010), pp. 673–689.
[23] P.M. Ramos, J.M. Dias Pereira, H.M. Geirinhas Ramos, and A.L. Ribeiro, *A four-terminal water-quality-monitoring conductivity sensor*. IEEE Trans. Instrum. Measure. 57 (2008), pp. 577–583.
[24] T. Messinger, *Comparison of storm response of streams in small, unmined and valley-filled watersheds, 1999–2001, Ballard Fork, West Virginia*. U.S. Geological Survey Water-Resources Investigations Report 02–4303, Charleston, WV, 2003.
[25] J.B. Wiley and F.D. Brogan. *Comparison of peak discharges among sites with and without valley fills for the July 8–9, 2001, flood in the headwaters of Clear Fork, Coal River Basin, mountaintop coal-mining region, southern West Virginia*. U.S. Geological Survey Open-File Report 03-133, Charleston, WV, 2003.
[26] C.T. Agouridis, C.D. Barton, and R.C. Warner, *Recreating a headwater stream system on a head-of-hollow fill: A Kentucky case study*, In Proceedings of Geomorphic Reclamation and Natural Stream Design at Coal Mines, Bristol, VA, 2009.
[27] C.T. Agouridis, C.D. Barton, and R.C. Warner, UT to Laurel Fork: Guy Cove (Hollow Fill #9) stream restoration monitoring report. Monitoring year 3: 2011. Submitted to the US Army Corps of Engineering, Louisville District, 2011.
[28] D.M. Grant, *ISCO open channel flow measurement handbook*, 3rd ed. ed., ISCO, Inc., Lincoln, NE, 1992.
[29] M.A. Cherry, *Hydrochemical characterization of the headwater catchments in eastern Kentucky*, M.S. Thesis, University of Kentucky, Lexington, KY, 2006.
[30] C.T. Haan, *Statistical methods in hydrology*, Iowa State University Press, Ames, IA, 1977.
[31] T. Kenny, *Sensor fundamentals*, in: *Sensor technology handbook*, J.S. Wilson, ed., Elsevier, Burlington, MA, 2005, pp. 1–20.
[32] SAS Institute, *SAS User's Guide*. Version 9. SAS Institute, Cary, NC, 2008.

[33] D.G. Kleinbaum, L.L. Kupper, A. Nizam, and K.E. Muller, *Applied regression analysis and other multivariable methods*, 4th ed. ed., Duxbury, Belmont, CA, 2008.

[34] C.B. Mastin, J.D. Edwards, C.D. Barton, A.D. Karathanasis, C.T. Agouridis, and R.C. Warner. *Development and deployment of a bioreactor for the removal of sulfate and manganese from circumneutral coal mine drainage*, in: *Bioreactors: Design, Properties and Applications*, P.G. Antollo and Z. Liu, eds., Nova Science Publishers, Hauppauge, NY, 2012, pp. 121–140.